

RESEARCH ARTICLE

Open Access



On-site monitoring for better selection of stone repairs: a case study

Thibault Demoulin¹ , Fred Girardet², Timothy P. Wangler¹, George W. Scherer³ and Robert J. Flatt^{1*}

Abstract

Weathering of clay-bearing sandstones does not only depend on material properties but also on the environmental conditions they are exposed to. The same is true for repaired stones, in which the compatibility of the repair mortar should be studied not only in terms of material properties, but also in terms of the climatic conditions it will be subjected, in order to maximize this compatibility. This paper proposes a methodology to quantify the thermal and hygric stresses in clay-bearing sandstones and their repair, based on the measurement of temperature and relative humidity at the surface and at several depths in a repaired and a non-repaired stone, as well as wind-driven rain and absorbed water. This is illustrated by a case study in an historical building. The data are used to quantify the stresses in the materials and to propose possible degradation mechanisms.

Keywords: On-site monitoring, Surface repair mortar, Acrylic-based mortar, Reprofilling, Sandstone degradation

Background

The durability of materials is the result of a combination of inherent material properties and of the action of the environment they are exposed to. There is therefore an intrinsic site-specific nature to any question of durability and this is something that requires particular attention in cultural heritage owing to the high value of the objects under consideration. The proper selection of repair materials has thus always been a major concern for conservators and continues to motivate much research and debate.

Modern technologies for on-site monitoring offer the possibility to address this issue much more efficiently, by acquiring site-specific exposure conditions. Combining such measurements with a material science approach to durability, it becomes possible to select materials by quantitatively accounting for case specific conditions.

This work presents such a methodology for studying the durability of clay-bearing sandstones used in historical masonry and their repair by a mortar. We illustrate this with a case study of a Swiss church erected partly

with sandstones and on which a specific repair mortar has been applied, for which questions about the material durability were to be examined.

Natural sandstone

The stone considered is a Swiss sandstone called molasse, mainly composed of quartz and feldspars cemented by calcite and clays [1–4]. The clays have been shown to be responsible for its large hygric and hydric swelling and to an increased softness in the wet state [5, 6].

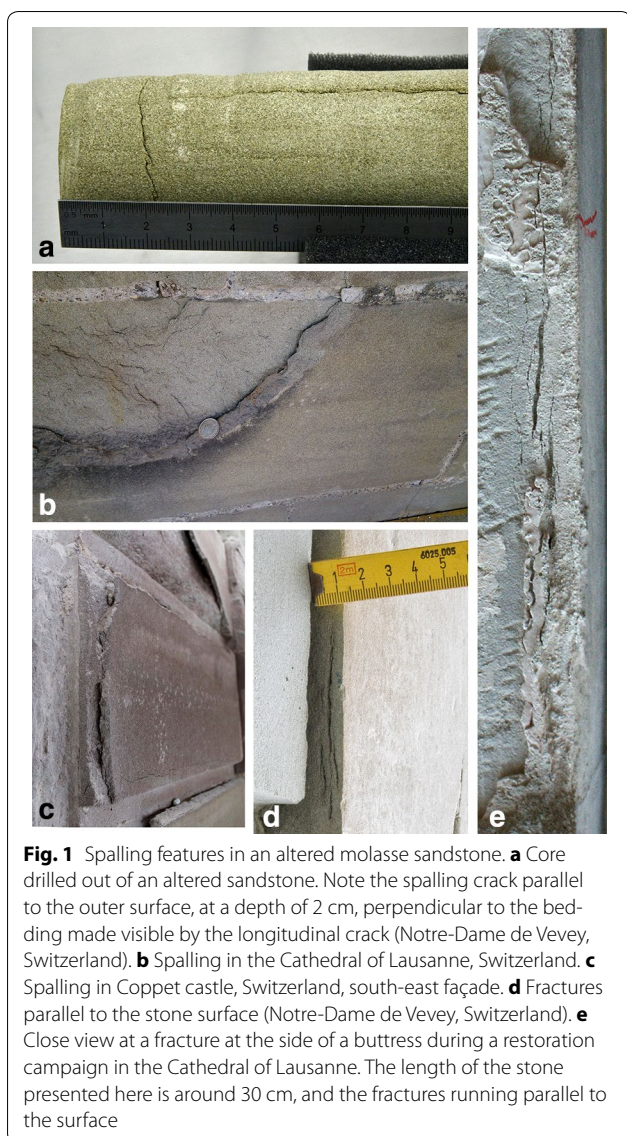
When used as a building stone, the molasse sandstone shows alteration patterns ranging from sanding to spalling of scales of several centimetres [7] depending on the exposure conditions [8–11]. When present, these degradations are all the more problematic in that they develop rapidly and require frequent restorations (for instance, every 50 years for the Cathedral of Lausanne [12]). However, they affect the stone only superficially, making the use of a repair mortar an interesting alternative to a full replacement by a substitution stone, in order to save as much historical material as possible.

The scales, the deepest damage morphology affecting the molasse sandstone, are formed parallel to the outer surface and are independent of the stone bedding orientation [6, 9, 13]. This is illustrated in Fig. 1a, with a core drill taken from the outer side of a wall of the church of

*Correspondence: flattr@ethz.ch

¹ Physical Chemistry of Building Materials, Institute for Building Materials, HIF, ETH Zurich, 8093 Zurich, Switzerland

Full list of author information is available at the end of the article



Notre-Dame de Vevey, Switzerland. The core shows a characteristic spalling crack parallel to the outer surface (2 cm deep in this case), but perpendicular to the bedding, which is on the longitudinal axis.

A closer look at the fracture indicates that several cracks can form parallel to each other, but always in a narrow range of depths (few millimetres), that they propagate parallel to the surface, and eventually coalesce. This suggests that the cracks can be initiated at several flaws in the stone and that the spalling is the result of several events that build up a stress large enough for the crack to propagate. That is depicted in Fig. 1d, e.

The scales are usually between 0.5 and 3 cm thick [13]. Underneath them one commonly finds a crumbling zone and flakes that can be dotted with efflorescences, as

shown in Fig. 1b, c. However, the thickness of the scales varies between stones as a function of their exposure. This has been reported in particular by Zehnder [9].

This suggests that a combination of physical properties and environmental conditions causes the stress of a degradation process to reach critical levels only at a certain depth. Deeper within, the stone is however in good conditions.

Acrylic-based repair mortar

When superficial alterations are observed, one option that a stone carver has to extend the lifetime of the historical material is to use a plastic mortar. “Plastic” here refers to the initial workability of the mortar, and not necessarily to a polymer content. Such a material is used as a small patch to retain the original shape of the stone after carving away degraded material. It is an interesting option when the preservation of the original material is the priority since it prevents the full replacement of stone blocks [14].

Cement and lime-based mortars were often used as reprofiling materials for molasse sandstone. In some cases, these repairs were judged totally inadequate for two main reasons: the differential colour evolution and the non-retreatability of the mortar, the later being the most problematic. For instance, in the Catholic Church of Notre-Dame de Vevey, Switzerland, the mortar was fixed with steel wires and screws to the stone, to anticipate a lack of adhesion to the substrate. As a consequence, removing the mortar required breaking a large part of the underlying molasse sandstone, which led to the opposite of the desired function of a reprofiling mortar, namely the extension of the lifetime of the historical material.

In an attempt to overcome these problems, an acrylic-based mortar was developed in the late seventies of the 20th century at the Ecole Polytechnique Fédérale de Lausanne in Switzerland. It is based on an acrylic resin that acts as a binder for the stone grains. It was applied on the townhall of Lausanne at this period and more than 30 years later the repairs are judged to be durable by the stone carvers. That is the reason why it has revived the interest of the practitioners and has been applied during the restoration of the church of Notre-Dame de Vevey in 2009.

However, the natural stone and the repair mortar studied here have very different physical properties, that are reported in Table 1. The natural stone is an Ostermundigen Blue sandstone, and the repair mortar is made by mixing crushed Ostermundigen Blue sandstone with a dispersion of Plextol D512 (Synthomer Deutschland GmbH, Marl, Germany).

The mortar displays a similar hygric swelling as the stone, but a much larger hygric swelling when in contact

Table 1 Properties of the materials

	Ostermundigen Blue sandstone	Repair mortar
Porosimetry (mercury intrusion porosimetry)		
Average pore radius (μm)	7.9	34.6
Total porosity (%)	17.2	35.1
Hygric swelling at 95% RH ϵ_{95} (mm m^{-1})	0.43	0.49
Hydric swelling ϵ_s (mm m^{-1})	1.25	5.02
Thermal expansion α (10^{-6}K^{-1})	12.9	32.7
Poisson's ratio ν (—)	0.2 ^a	0.4 ^b
Elastic modulus E (GPa)		
Wet	0.43	—
Dry	1.87	2.03
Relaxation modulus		
Dry	—	$E_0 \exp(-(t/\tau)^\beta)^c$
Tensile strength (MPa)		
Wet	0.3	—
Dry	1.0	2.7

The Ostermundigen Blue is a sandstone largely used in built heritage in Switzerland, and the repair mortar studied here is made by mixing the powder of this stone with an acrylic resin

^a Taken from [18]

^b Taken from [19]

^c With E_0 the instantaneous elastic modulus of the stone (2.03 MPa), t the time in s, τ the temperature-dependent relaxation time ($4.87 \times 10^{-59} \exp(\frac{3.94 \cdot 10^4}{T}) \text{s}$) and β an exponent equal to 0.206 [20]

with liquid water, as shown in Fig. 2. However, their kinetics are very different: while the stone expands in few minutes when in contact with water, the mortar reaches the same value only after 3 h. A longer immersion would result in the mortar swelling four times more than the stone. This is shown in Fig. 3.

The thermal expansion coefficient of the mortar is also nearly three times higher.

A series of questions thus arise about possible incompatibilities between the neighbouring natural and artificial stones after restorations are completed. In particular, how the differential thermal, hydric and hygric properties affect the durability of the repair and, more importantly the state of the underlying stone have not yet been examined systematically.

The topic of compatibility between repair mortars and historic substrates has received great attention, and led to the definition of guidelines for successful repairs [15–17]; however, they have mainly been defined considering mineral binders.

Due to the polymeric nature of the binder, the mortar features marked viscoelastic properties associated

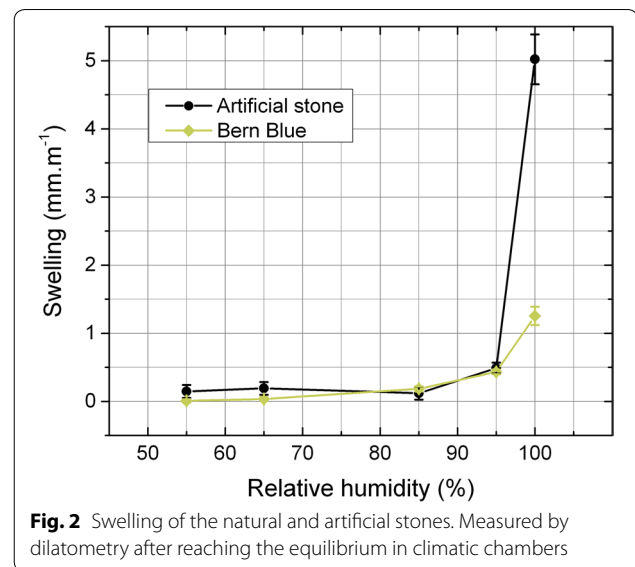


Fig. 2 Swelling of the natural and artificial stones. Measured by dilatometry after reaching the equilibrium in climatic chambers

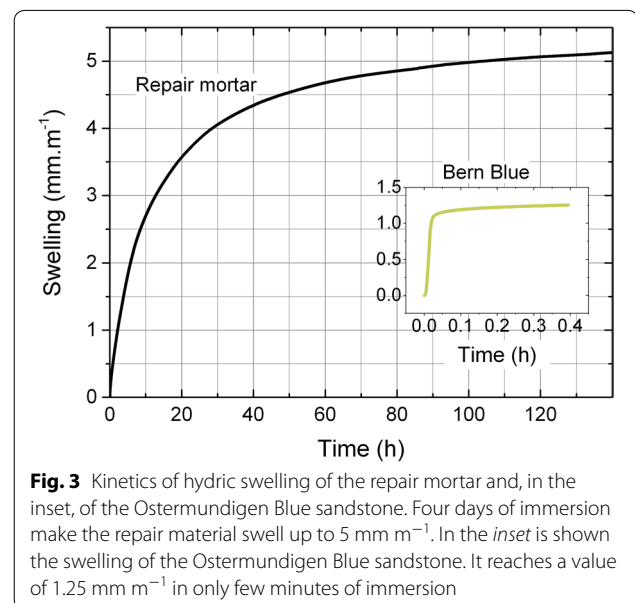


Fig. 3 Kinetics of hydric swelling of the repair mortar and, in the inset, of the Ostermundigen Blue sandstone. Four days of immersion make the repair material swell up to 5 mm m^{-1} . In the inset is shown the swelling of the Ostermundigen Blue sandstone. It reaches a value of 1.25 mm m^{-1} in only few minutes of immersion

with a low glass transition temperature of 20°C . This has important consequences for the development of stresses in the repair.

The stresses that can develop in the natural stone and a repaired stone are evaluated according to the possible degradation mechanisms proposed in the following section.

Background on the mechanisms of degradation

Let's first consider the case of a natural stone used in a masonry. When exposed to the action of the environment, whether mist, rain or warming by the sun, it may

be submitted to large dimensional changes. Since materials act as a filter that buffers the fluctuations of these stimuli, their surface is prone to high dimensional changes while their core is exposed to less variations. The surface is thus restrained by the core, a situation known as “self-restraint”, and this leads to mechanical stresses at a depth and of a magnitude dictated by the environmental conditions.

Let’s imagine a stone in a masonry during a rain event. Before the rain, the stone is dry. The rain starts wetting the stone, forming a thin layer of wet stone that is prevented from expanding by the thick layer of dry stone [5]. This situation is illustrated in Fig. 4a–c. If the stone is considered as a purely elastic material, and if the thickness of the superficial layer is very small compared to the thickness of the core, the resulting stress created in the superficial layer is written [5]:

$$\sigma_{wet} = \frac{E_{wet}}{1 - \nu_{wet}} (\epsilon_{RH} - \epsilon_s) \tag{1}$$

where E_{wet} and ν_{wet} are respectively the elastic modulus and the Poisson’s ratio of the wet stone, ϵ_s its free swelling strain and ϵ_{RH} the strain of the dry stone in equilibrium at a certain relative humidity. Here, $\sigma_{wet} < 0$ so the stress is compressive. This is expected to be a problem if the stress is larger than the compressive strength of the wet stone. However, if the stone contains pre-existing defects below the surface, buckling of the stone above the defect could happen at a stress lower than its compressive strength. This will be discussed later.

If the rain continues wetting the stone, the water is transported through it until the rain stops and the stone begins to dry. This will form a thin layer of dry stone restrained from shrinking by a large layer of wet stone, situation depicted in Fig. 4d–f. The stress created in this thin layer is described by the following equation [5]:

$$\sigma_{dry} = -\frac{E_{dry}}{1 - \nu_{dry}} (\epsilon_{RH} - \epsilon_s) \tag{2}$$

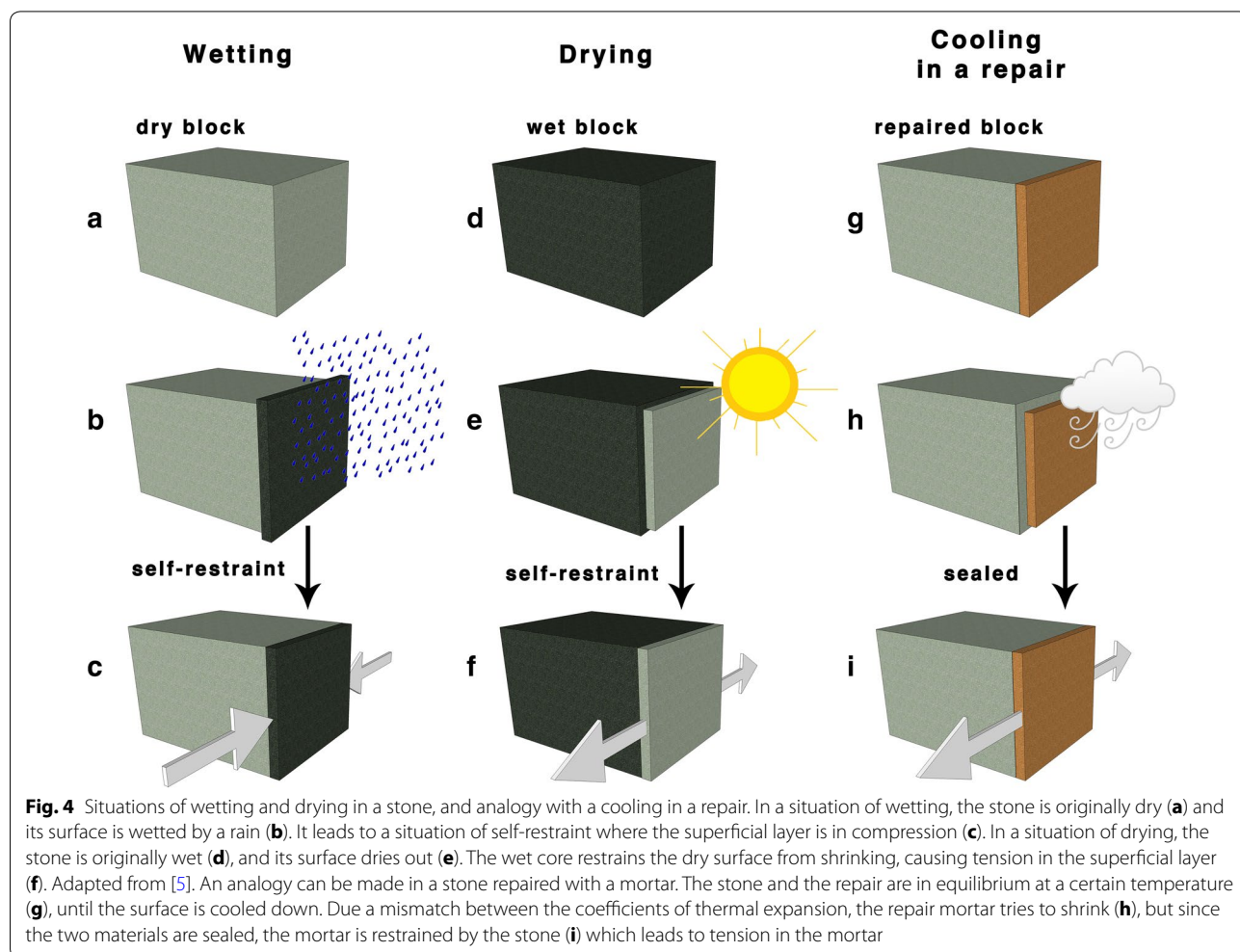


Fig. 4 Situations of wetting and drying in a stone, and analogy with a cooling in a repair. In a situation of wetting, the stone is originally dry (a) and its surface is wetted by a rain (b). It leads to a situation of self-restraint where the superficial layer is in compression (c). In a situation of drying, the stone is originally wet (d), and its surface dries out (e). The wet core restrains the dry surface from shrinking, causing tension in the superficial layer (f). Adapted from [5]. An analogy can be made in a stone repaired with a mortar. The stone and the repair are in equilibrium at a certain temperature (g), until the surface is cooled down. Due a mismatch between the coefficients of thermal expansion, the repair mortar tries to shrink (h), but since the two materials are sealed, the mortar is restrained by the stone (i) which leads to tension in the mortar

where E_{dry} and ν_{dry} are respectively the elastic modulus and the Poisson's ratio of the dry stone. In this case, the stone is in tension. Since the stone is much weaker in tension than in compression, the drying event could be more damaging for the stone, as pointed out by Jiménez-González et al. [18] who calculated that this stress has the potential to overcome the tensile strength of the dry stone.

The situations of wetting and drying can be transposed in term of heating and cooling. Temperature variations at the surface of the stone create a gradient of temperature in the wall that can lead to the formation of stresses, acting at the boundaries of the grain minerals [21, 22]. For instance, if a thin region at the surface of the stone is cooled down while the inner part of the stone remains warm, the above-mentioned hygric equation can be transformed into the following:

$$\sigma_{cooling} = -\frac{E}{1-\nu}\alpha(\Delta T) \quad (3)$$

where α is the coefficient of thermal expansion of the stone and ΔT is the temperature difference between the surface layer and the core of the stone.

The above-mentioned situations create stress by a mechanism of "self-restraint" because there exist, in the same material, two layers that try to adopt different states of strain.

The same analysis can be extrapolated to a reprofiled stone, which can be seen as a thick layer of stone covered by a thin layer of repair mortar, as depicted in Fig. 4g–i. In this case, the layer of repair material will try to adopt a strain but will be prevented from doing so by the thick underlying layer of original stone that will instead impose its strain and cause subsequent stresses in the repair. This is relevant considering the large expansion differences (thermal or hygric) between the repair mortar and the natural stone listed in Table 1.

The mortar considered in this paper is viscoelastic and thus possesses temperature and time-dependent mechanical properties. Consequently, the stresses that can arise in the mortar and the stone to be repaired are a complex problem depending on the following factors:

1. The dilatation coefficient of each material;
2. Their respective thicknesses;
3. Their respective elastic moduli;
4. The proximity of the temperature of the acrylic-based mortar to its glass transition (here, 20 °C), which governs its viscoelastic properties;
5. The complete history of the stimulus (seasonal and daily variations of the temperature and the RH);
6. The rate at which these variations occur.

For instance, due to the large thermal expansion mismatch, temperature may a priori represent a non-negligible source of stresses in the repair. These thermal stresses have to be formulated by considering its viscoelastic properties. In the following equations, the subscript p (patch) is used to describe the repair mortar. The thermal stresses can be written:

$$\sigma_p = \frac{E_p}{1-\nu_p} [\psi_0(\varepsilon_{f,s} - \varepsilon_{f,p}) + (1 - \psi_0)(\alpha_s \Delta_s - \alpha_p \Delta_p)] \quad (4)$$

where E_p is the instantaneous elastic modulus of the patch and ν_p the Poisson's ratio of the patch, ψ_0 the residual fraction of the stress that does not relax, $\varepsilon_{f,p}$ and $\varepsilon_{f,s}$ the free strain of the patch and the stone, α_s and α_p are the coefficients of thermal expansion of the stone and the patch.

Δ_s and Δ_p are the integrals that consider the difference of temperature between the two materials (as the massive wall responds more slowly to environmental changes than the thin patch) and are written:

$$\Delta_s = \int_0^t \exp \left(- \left(\int_{t'}^t \frac{dt''}{\tau_0 \exp \left(\frac{Q}{T_p [t'']^{\beta}} \right)} \right)^{\beta} \right) \frac{dT_s}{dt'} dt' \quad (5)$$

and

$$\Delta_p = \int_0^t \exp \left(- \left(\int_{t'}^t \frac{dt''}{\tau_0 \exp \left(\frac{Q}{T_p [t'']^{\beta}} \right)} \right)^{\beta} \right) \frac{dT_p}{dt'} dt' \quad (6)$$

where τ is the relaxation time and β an exponent ($0 < \beta < 1$).

The complete analysis leading to these equations can be found in [20].

Knowing the conditions of temperature and humidity is thus a prerequisite to obtain a more comprehensive understanding of the compatibility between the repair mortar and the historical stone, and of the processes leading to their degradation.

The next section describes the equipment used to acquire these data.

Methods

The approach proposed is illustrated with a measurement campaign that extended from July 2013 to September 2015 in the church of Notre-Dame de Vevey, in Switzerland. This church underwent an extensive restoration campaign from 2009 to 2011 where part of the altered sandstones were repaired using the acrylic-based mortar, while others, in which the alterations were too large, were repaired with a substitution sandstone. This gave us the

possibility to study the conditions to which both repaired and non-repaired stones are exposed, and to quantify the frequency and the magnitude of the above-mentioned situations. In that process, two locations, shown in Fig. 5, were selected: the first in a buttress and the second in the tower of the church.

The measurement in the buttress was dedicated to the study of a repaired stone, and compared with a stone that was not repaired. In addition, wind-driven rain sensors were installed to quantify the amount of water absorbed by the two materials.

The tower of the church, unusually, is entirely built with molasse blocks of around 30 cm thick. It offers the possibility to study the sandstone alterations at four cardinal points.

These two locations were equipped with sensors of temperature (T) and relative humidity (RH). The availability on the market of robust and autonomous sensors of small size makes it possible to develop relatively non-invasive instrumentation that measures at different depths in the material, and which can be abandoned in a wall for several weeks [23, 24].

The apparatus used in each case is described below. The data obtained and the expected stresses are analysed in “Results and discussion” section, using equations described in the previous section.

Measurements in the buttress

Monitoring the temperature and relative humidity

The measurement is subject to two constraints:

1. Finding a location where the sensors can physically be installed. This task is made challenging due to the large size of the rain sensors (26 cm × 26 cm × 26.7 cm),

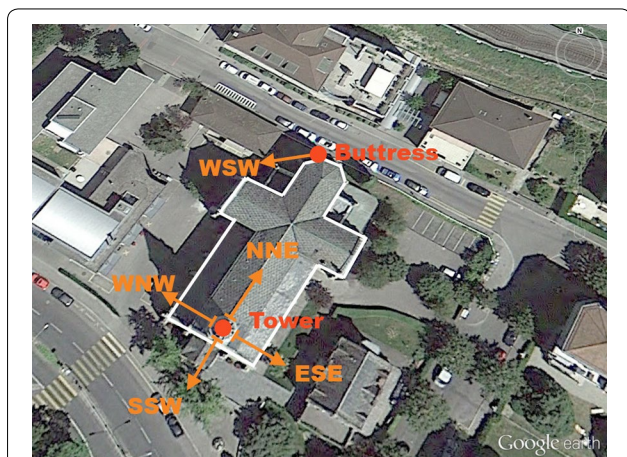


Fig. 5 Top view of the church of Notre-Dame de Vevey, Switzerland. The church is delimited by white lines, the two locations (buttress and tower) are displayed with their respective exposure

2. Finding an appropriate exposure that might be particularly harsh for the stone.

The location that best satisfied these requirements was found on a buttress of an apse, approximately 6 m above the ground, where relatively large areas of stone were repaired using the acrylic-based mortar, as seen in Fig. 6. These repairs are actually larger than typical reprofiling patches.

The measurements were done on the molasse sandstone and on an adjacent block of the same stone reprofiled with a layer of repair material. Figure 6 shows the proximity of the measurements, with the dimensions of the repair layer (12 cm width and 26 cm height for 2 cm thickness).

Two sets of sensors are used, one in the natural stone and one in the repaired stone. They measure T and RH at the surface and at different depths in the wall. They are detailed in Fig. 7.

To measure at different depths, several loggers are put together and separated by expanded polyvinyl chloride (PVC), a material with a low thermal conductivity ($0.06 \text{ W m}^{-1} \text{ K}^{-1}$ against $2.30 \text{ W m}^{-1} \text{ K}^{-1}$ for the molasse). The loggers (grey discs) are shown in Fig. 7a. They are mounted together with the expanded PVC (white material). Each of the sensors is connected with thin wires to allow remote access, and the whole is protected in a polyolefin shrink-fit tube. The sensors are inserted in the wall and record the data at depths of 1.0, 2.5, 4.0 and 6.7 cm. In the case of the repaired stone, they allow measurement in the repair mortar at 1 cm, and in the stone substrate at 2.5, 4.0 and 6.7 cm, as schematised in Fig. 6.

The sensor measuring T and RH in the air is positioned a few centimetres from the wall to record the direct environment of the building. It is protected from the direct sun radiation by a white screen, as illustrated in Fig. 7c.

The sensors applied at the surface of the materials are encapsulated in expanded PVC, and the thermal contact is ensured by a metallic washer. To protect the volume of air limited by the washer from the intrusion of contaminants like salts, that could perturb the measurement of humidity, the washer is surrounded by a filter of polytetrafluoroethylene (PTFE). One of these sensors is shown in Fig. 7d.

The T and RH sensors are capacitive Hygrochron loggers (Maxim Integrated, San Jose, CA, USA) that function through the 1-Wire protocol. This allows having as many wires as sensors plus one for the ground, hence keeping as low as possible the physical impact of the measurement that could be deteriorated by water infiltration or thermal heating of the wires. Moreover, each sensor being autonomous, the need for a central acquisition

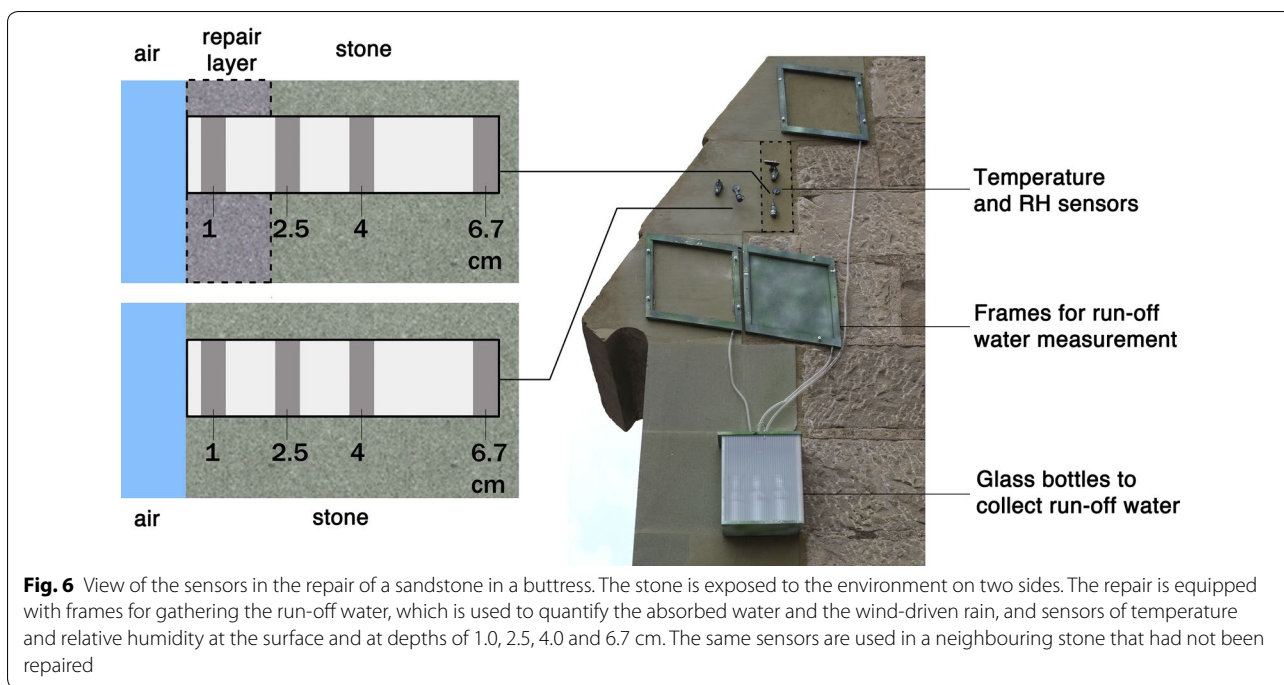


Fig. 6 View of the sensors in the repair of a sandstone in a buttress. The stone is exposed to the environment on two sides. The repair is equipped with frames for gathering the run-off water, which is used to quantify the absorbed water and the wind-driven rain, and sensors of temperature and relative humidity at the surface and at depths of 1.0, 2.5, 4.0 and 6.7 cm. The same sensors are used in a neighbouring stone that had not been repaired

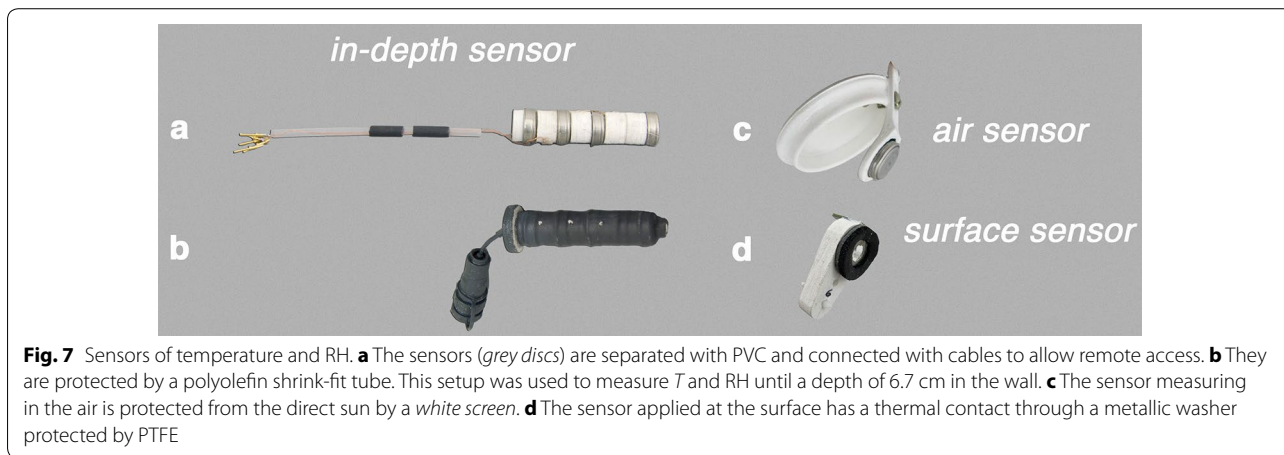


Fig. 7 Sensors of temperature and RH. **a** The sensors (grey discs) are separated with PVC and connected with cables to allow remote access. **b** They are protected by a polyolefin shrink-fit tube. This setup was used to measure T and RH until a depth of 6.7 cm in the wall. **c** The sensor measuring in the air is protected from the direct sun by a white screen. **d** The sensor applied at the surface has a thermal contact through a metallic washer protected by PTFE

system is avoided, thus reducing the invasive nature of the installation.

The sensors measure $-20 > T (^{\circ}\text{C}) > 85$ with a resolution of $0.06\text{ }^{\circ}\text{C}$ and an accuracy of $0.5\text{ }^{\circ}\text{C}$ between -10 and $65\text{ }^{\circ}\text{C}$, that exceeds the range observed during the campaign. The RH is measured from 0 to 90%, with an accuracy of 2% within $0 < T (^{\circ}\text{C}) < 50\text{ }^{\circ}\text{C}$ that were mostly the conditions encountered during the campaign. Accuracy in the measurement of $\text{RH} > 90\%$ however decreases to 5%.

The measurement campaign in this location lasted from July 2013 to July 2014.

Monitoring the rain events

During a rain event, the rain driven to the stone by the wind can be either absorbed by the stone or run off its surface. Since water transport is of utmost importance in stone degradation, the behaviour of both artificial and natural stones during rain events must be quantified. To this end, the horizontal rainfall, the wind-driven rain and the run-off water are measured. The difference between the two last quantities gives the amount of water absorbed by the stone. The complete apparatus used for the measurements is visible in Fig. 6 and a close-up view is given in Fig. 8.

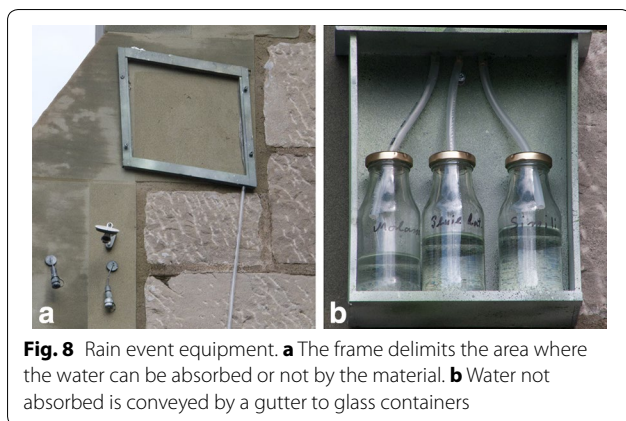


Fig. 8 Rain event equipment. **a** The frame delimits the area where the water can be absorbed or not by the material. **b** Water not absorbed is conveyed by a gutter to glass containers

Run-off water is measured through the collection of the water flowing over an area delimited by a frame (0.069 m²), at the surface of the natural and the artificial stone. The wind-driven rain is quantified using the same equipment, but the surface of the stone is covered by a fully non-absorbing material. The water is collected in glass bottles and weighed; the sampling rate is thus determined by the frequency of the weighing done by an operator. In a more recent project, this system has been updated with automated measuring devices, but was not available for this measurement campaign.

Measurements in the tower

The tower has the advantage of being free from the influence of the neighbouring buildings due to its height. Four sets of sensors were positioned at the surface of the stone and at a depth of 4 cm from the surface. One of them is shown in Fig. 9. The sensors at the surface were similar to the ones used in the buttress, while the sensors in-depth were capacitive Sensirion CMOS SHT15 sensors (Sensirion, Stäfa, Switzerland) measuring the temperature with an accuracy of ± 0.3 °C and the RH with an accuracy of $\pm 2\%$ in a range of 10–90%, and $\pm 4\%$ above this. The sensors were installed in stones facing North–North–East, East–South–East, South–South–West and West–North–West, as they were the only set of stones that were reasonably easily accessible. The measurement in the tower covers a period from July 2014 to July 2015.

Results and discussion

Natural stone

Influence of the exposure

The measurement at four cardinal points in the tower exemplifies the very different thermal and hygric regimes to which the stones are exposed, and which lead to different alteration patterns. Spalling of flakes is indeed generally found on the surfaces exposed both to the rain and to

fast drying, while sanding appears preferentially in humid locations with slow drying [9].

The results obtained during a period of one year from July 2014 to July 2015¹ are summarized in Fig. 10, and the data on which this figure is based are reported as Additional file 1.

The apparent motion of the sun allows for a long heating of the stone during winter time in the southern and to a smaller extent in the eastern locations, but does not reach the western side. The latter is heated by the sun when spring comes. On the contrary, the sun never heats the northern location much, so there the temperature of the stone follows the temperature of the air. This has several consequences in terms of temperature and RH in the stone.

Three exposures are clearly more prone to high daily temperature variations: the southern, the western and the eastern experienced daily temperature variations of more than 23 °C against 15 °C for the northern exposure. The same trend can be found for the yearly temperature variations, which are of only 30 °C for the northern exposure while around 38 °C for the others.

Concerning the RH, Fig. 10 shows the drastic difference that exists between the Southern and the Northern exposures: at a depth of 4 cm, the stone remains wet/very humid 92.6% of the time in the NNE while only 23.4% of the time in the SSW. The Northern exposure (NNE) is thus a very humid location with low temperature variations; the Southern exposure (SSW) is dryer and exposed to high temperature amplitudes. The Eastern (ESE) and Western (WNW) orientations are variations of the two previous ones, with the Western one characterized by a very humid/wet stone (90.7% of the time) with high amplitudes of daily temperature variations, and the Eastern one sensibly dryer but also exposed to high temperature variations.

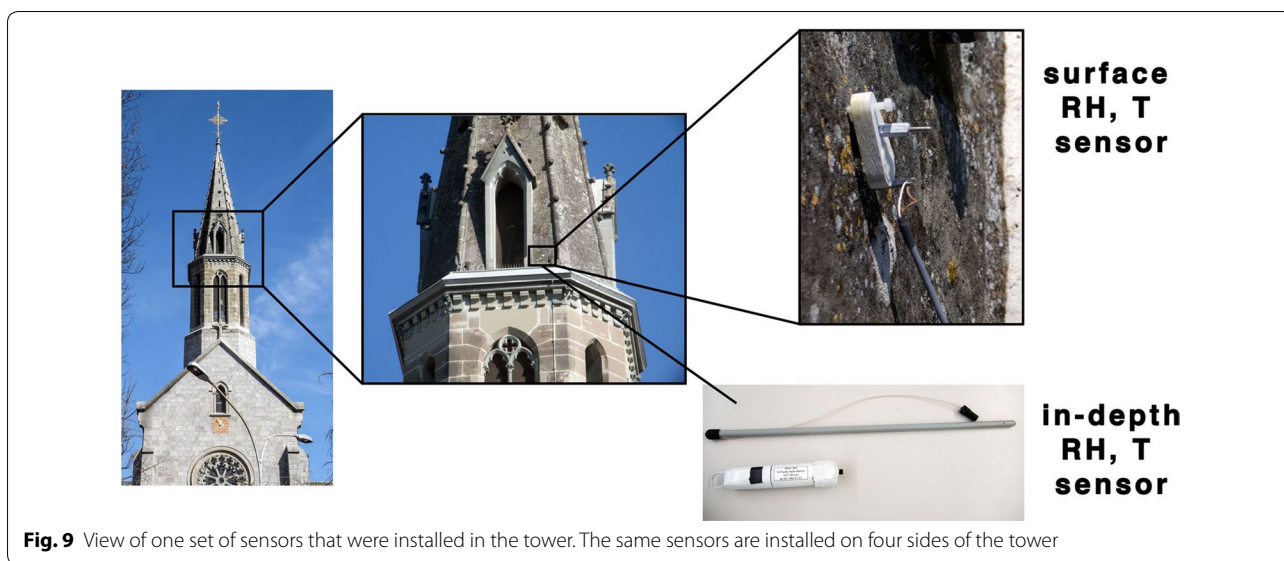
These differences re-emphasize the importance of the local monitoring to develop a more comprehensive view of the situations that may lead materials to fail or not at given sites.

The following sections aim at evaluating the stresses that arise from these variations of *T* and RH in the stone, measured at a particular location: the buttress, facing West–South–West.

Influence of the temperature

Temperature is a driving factor in stone weathering processes such as salt crystallization and wetting/drying cycles. However, the question of whether it is a factor of degradation per se, apart from extreme events like frost or fire, is

¹ Except the months of August and September 2014 when the sensors were not recording.



still a subject of debate [25]. Here, we examine whether a large temperature difference throughout the wall might lead to damaging stresses via situations of self-restraint.

Fast heating and cooling take place at the stone surface, but the thermal properties of the stone buffer the temperature variations and lead to temperature gradients throughout the wall. Figure 11 shows that in the first centimetre of the stone, the temperature gradient can be more than 5 times higher than at a depth of 2.5 cm.

The most extreme situation encountered during the measurement campaign is one of cooling presented in Fig. 12 which led to a temperature difference of 4.1 °C

between the outer layer (0.5 cm) and the deepest point measured (6.7 cm). According to Eq. 3, this yields a tensile stress of 0.1 MPa, namely 10% of the tensile strength of the sandstone (1 MPa). It thus precludes rapid failure in such thermal cycles.

Influence of the humidity

The humidity in the air and in the stone during the measurement period is shown in Fig. 13.

This shows that the RH in the air is on average lower in spring and summer than in autumn and winter, but is still subject to high and fast variations throughout the

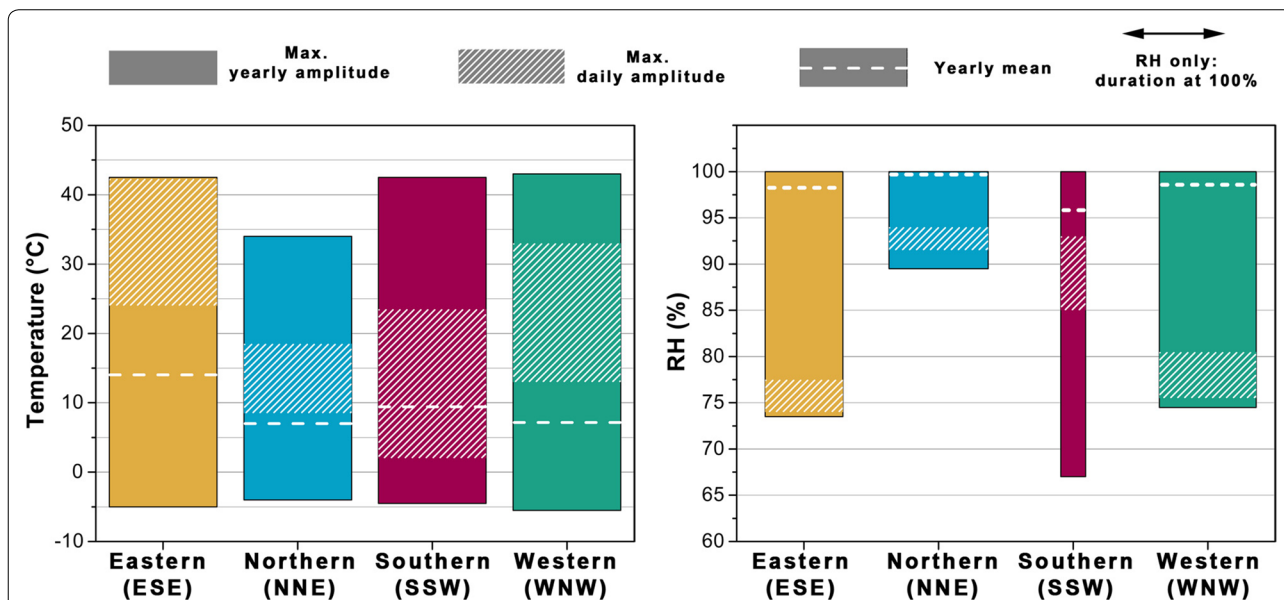


Fig. 10 Temperature and RH observations measured on the different exposures. Measured at a depth of 4 cm over a period from July, 25th 2014 to July, 25th 2015*. *ESE* stands for East–North–East, *NNE* for North–North–East, *SSW* for South–South–West and *WNW* for West–North–West

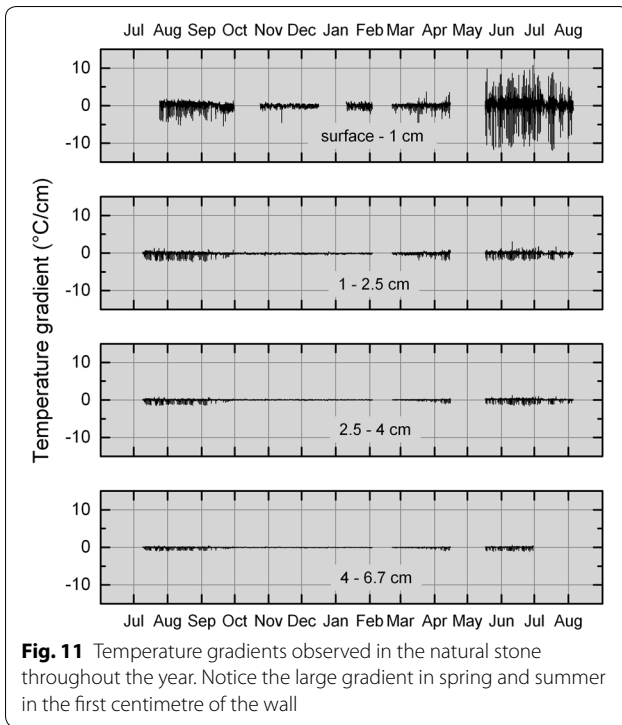


Fig. 11 Temperature gradients observed in the natural stone throughout the year. Notice the large gradient in spring and summer in the first centimetre of the wall

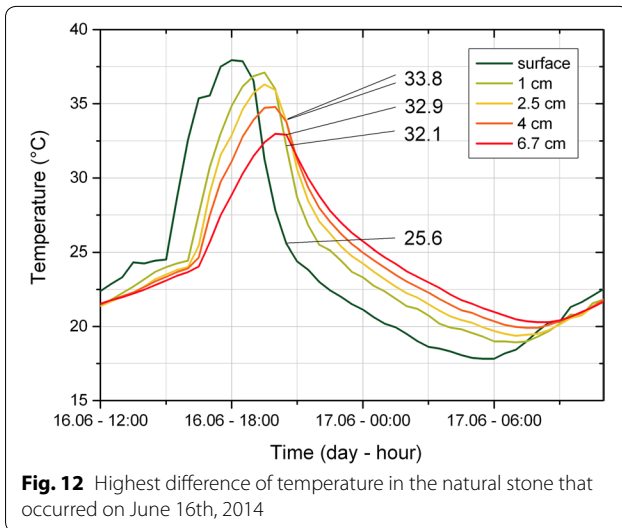


Fig. 12 Highest difference of temperature in the natural stone that occurred on June 16th, 2014

whole year. The maximum RH was, as one can expect, 100%, while the lowest value recorded was only 19.5% after a particularly dry week at the beginning of September 2013.

In the stone, the highest fluctuations of RH take place at the surface, when rain suddenly wets a previously dry stone. However, the RH below the surface varies much less and stays relatively high. Indeed, at a depth of 4 cm for instance, during the course of one year the humidity

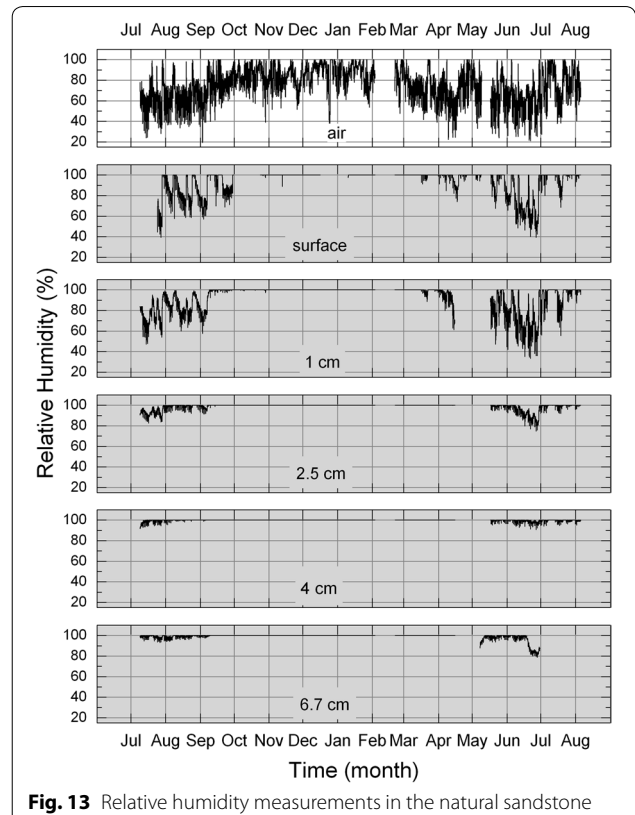


Fig. 13 Relative humidity measurements in the natural sandstone

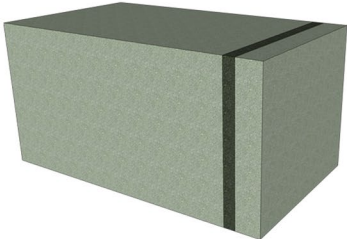
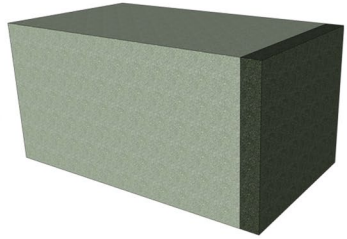
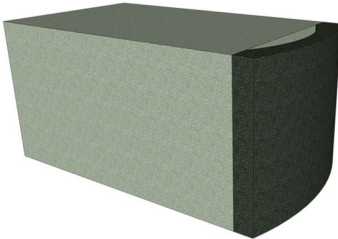
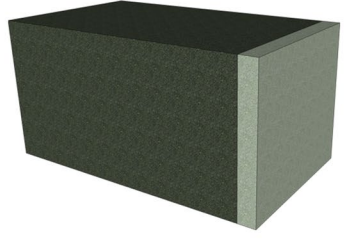
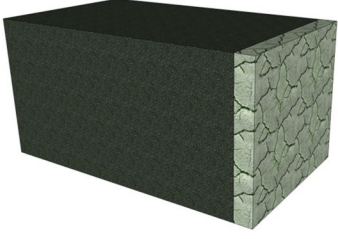
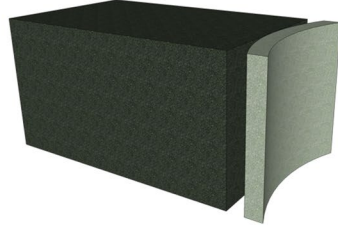
did not fall below 90%, while the mean humidity was 99.8, and 90% of the time it remained at 100%.²

The RH in the stone is thus close or equal to 100% for a large part of the year. We reach here the limitation of the sensors that are dedicated to the measurement in the hygric regime, and suffer from a large inaccuracy ($\pm 5\%$) at high humidities. In other words when we measure 100% RH, the stone may or not be fully saturated. Also, if not fully saturated its humidity could be between 95 and 100% RH. Unfortunately, this is also the range in which the swelling increases exponentially as shown for our stones in Fig. 2, and with a higher accuracy in other clay-bearing sandstones in [26].

As a result, swelling strains on site cannot be determined accurately in that range, and this must be taken into discussing damage mechanisms as those summarized, and to evaluate their role in the degradation of the sandstone in this specific site. Four situations have been measured on-site and are described in Table 2; each of them is detailed below.

² This period though does not include the months of February and May, due to technical issues.

Table 2 Scheme of the situations measured in the stone and the expected damage mechanisms they could induce

Situations that can potentially lead to damage	Description	Expected damage mechanisms
<p>a</p> 	<p>Internal wet layer between 2.5 and 6.7 cm</p>	<p>Fatigue through swelling cycles, initiation of defects through salt crystallization at the drying front</p>
<p>b</p> 	<p>Wet surface on the first cm</p>	 <p>Buckling if flaws are present</p>
<p>c</p> 	<p>Dry surface on the first cm</p>	 <p>Mud-cracking</p>  <p>Peeling if flaws are present</p>

Note that the schemes represent the whole block, but only a depth until 6.7 cm has been investigated; the hygric state of the rest of the stone is extrapolated from the deepest measurement done

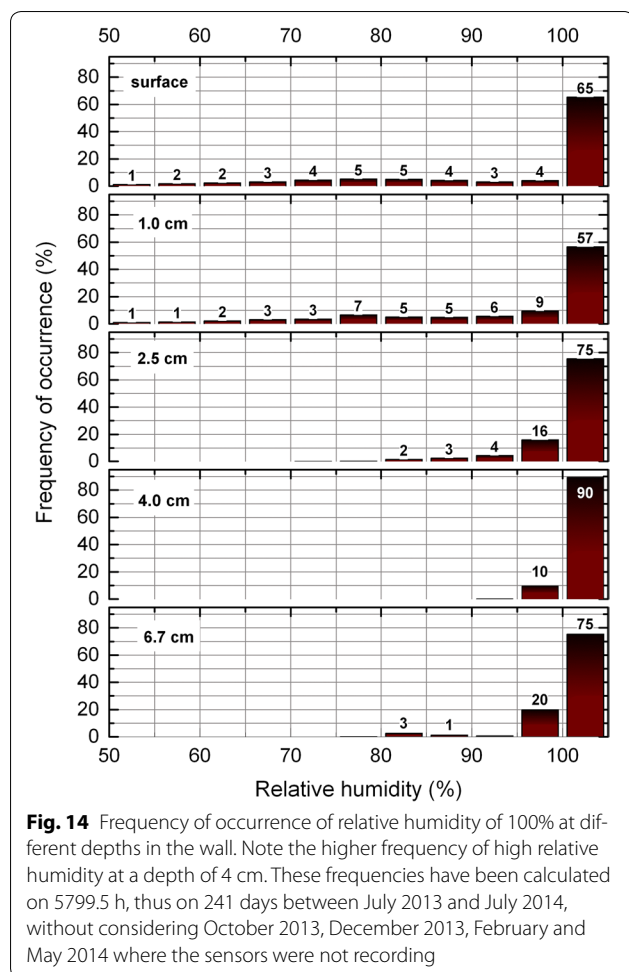
Internal wet layer

Our measurement highlights a singularity at a depth of 4.0 cm, the presence of an internal layer in the stone where the RH stays at 100% much longer. As shown in Fig. 14, this was the case for 90% of the time against 75% for the depths of 2.5 and 6.7 cm. This situation is depicted in Table 2a.

Consequently, there is a zone that can dry out towards the surface but also towards the inside of the stone, and remains wet longer. This has already been discussed by Sneath and Wendler who presented modelling results in this sense

[27]. To the best of our knowledge direct experimental measurements for this were not previously reported.

The presence of this wet zone is important as it might explain the weakening of the clay-bearing stone at a characteristic depth. It could indeed lead to an enrichment of salts at this particular location. In this respect, it can be put in relation with measurements made by Zehnder on molasse sandstone. By investigating the deleterious effect of sulphur deposition in the stone, he found that in locations frequently exposed to rain the distribution



of sulphur had a maximum between 2 and 5.5 cm, but sharply decreased below it [10].

The presence of a wet layer could thus favour stresses from salt crystallization or freezing to occur at a certain depth, and which may lead to the initiation of defects in the stone. However as scaling degradation is also observed in tropical climates [28], freezing cannot be advanced as a necessary condition.

Furthermore, the propagation of cracks from these defects and in this plane could be favoured due to the relatively smaller toughness of the wet stone compared to a drier one [29]. It would involve mechanisms that could lead to the propagation of fractures at a stress lower than the tensile or compressive strength of the stone and that are discussed below.

Wetting situation

The data of Fig. 13 indicate that the core of the stone remained at 100% RH more than half of the year, and that this tendency is more pronounced in depth. For the site considered, this implies that situations of surface wetting

presented in Table 2, where the core of the stone is dry while the outer first centimetre is wet, happens rarely (0.05% of the time, on the close to 6000 h monitored). However, given the accuracy of the sensors in this range of RH, there may be situations where the outer layer is wet and fully saturated, while the core is only “very humid”.

The restrained swelling of the wet layer is the difference between the strain of the dry layer (the lowest RH recorded is 95%) and the free swelling strain of the saturated stone. It amounts to 0.82 mm m^{-1} . According to Eq. 1, it could lead to a maximum compressive stress in the wet layer of 0.44 MPa. This is much lower than the wet compressive strength expected for the Ostermundigen Blue ($\sim 3.2 \text{ MPa}$, considering a factor 10 with respect to the dry strength of 32 MPa [30]).

However, compressive stresses could provoke the concentration of tensile or shear stresses at the tip of a pre-existing crack, that would propagate fracture at much lower stress value. Wangler et al. [31] demonstrated that inhomogeneous wetting could lead to flaw growth, by creating bending moments due to local swelling, if the wet region is comparable in size to the flaw. That would ultimately lead to buckling as illustrated in Table 2. Typical buckling morphologies are however not commonly found in the church of Vevey.

Drying situation

A damage morphology observed more often in Vevey is shear delamination starting at the edges of the stone blocks. These are related to tensile rather than compressive failure, and are most probably caused by drying.

The situation of surface drying, the second scheme in Table 2, appears to be common since the stone remains at $\text{RH} = 100\%$ a large part of the time. A drying event is here considered to occur when the humidity decreases below 100% in the outer centimetre, while it remains at $\text{RH} 100\%$ at a depth of 2.5–6.7 cm. Such events were represented 6.7% of the time monitored. Considering a RH at 0.5 cm of 68.3% (obtained by linear interpolation between the values of RH at the surface and 1 cm), leads to a restrained strain of 1.19 mm m^{-1} in the superficial layer, and to a maximum tensile stress of 2.8 MPa. Owing to the inaccuracy of our sensors at high RH, the stone may not be fully expanded when 100% RH is measured. RH could be about 95%, which would reduce the restrained strain to about a third and lead to a tensile stress of 1.0 MPa.

The stress calculated above is in the order of the tensile strength of the stone (1 MPa), which suggests that it could get damaged during drying events. Two patterns could thus be expected to develop: a so-called “mud-cracking” pattern due to desiccation cracks perpendicular to the surface, often seen in desiccating mud [32],

and/or a peeling pattern that would lead to cracks parallel to the surface and eventually to the delamination of curled layers [33].

The mud-cracking pattern is usually not reported on-site in molasse sandstone, except in protruding elements that can become fully wet and fully expanded before drying. However, this is not seen on a façade. This could be due to the development of a moisture gradient during drying, that would reduce the maximum stress.

However, it could also mean that delamination may prevail, in which the propagation of pre-existing cracks parallel to the surface would occur before the formation of perpendicular cracks. The tension in the dry layer is biaxial, so the greatest mode I stress would tend to open cracks perpendicular to the wet/dry boundary (mud cracks). Nevertheless, if there is a large horizontal flaw, it might grow instead parallel to the surface, even though it is only driven by mode II stresses. This is schematized in Fig. 15a, b. Eventually, the crack would reach the edge of the stone, and drying stresses would create a bending moment that would tend to separate the thin layer from the substrate, and open a mode I crack, like in Fig. 15c.

This last step, referred to as peeling, would ultimately lead to spalling of concave layers. This can be observed in drying muds and had been studied by Style et al. [33].

This morphology corresponds to the one sometimes seen in molasse sandstone, a concave plate shown in Fig. 1c. This is why this damage mechanism should be seriously followed-up.

In the repair

Temperature in the repair

In the repair, the temperatures that matter the most are those measured in the mortar and in the stone below it, since they govern the strains and stresses that can develop in these materials. Consequently, in Fig. 16 we only report the temperatures measured in the mortar at a depth of 1.0 cm (b) and in the natural stone it covers at 2.5 cm (c) in addition to the air temperature (a).

The seasonal variations occurring throughout 1 year inform about the minimum and maximum service temperature to which the materials are confronted, and thus to their minimum and maximum strain, through the following formula:

$$\varepsilon = \alpha \Delta T \quad (7)$$

where ε is the strain, α is the coefficient of thermal expansion and ΔT the temperature variation.

From the data of Fig. 16, temperature at the surface of the repair material varied from -2 to 43.1 °C. This could induce an overall dimensional change of 1.46 mm m^{-1} . In the stone below the repair layer, temperature varied from -0.9 to 39.7 °C, leading to a dimensional change of 0.52 mm m^{-1} . The repair layer is thus subjected to a higher temperature variation, and moreover, having a higher coefficient of thermal expansion, seeks to achieve a higher dimensional change.

The daily temperature variations can lead to large temperature differences between the repair material and the underlying natural stone over a much shorter period of time. The associated daily temperature amplitudes

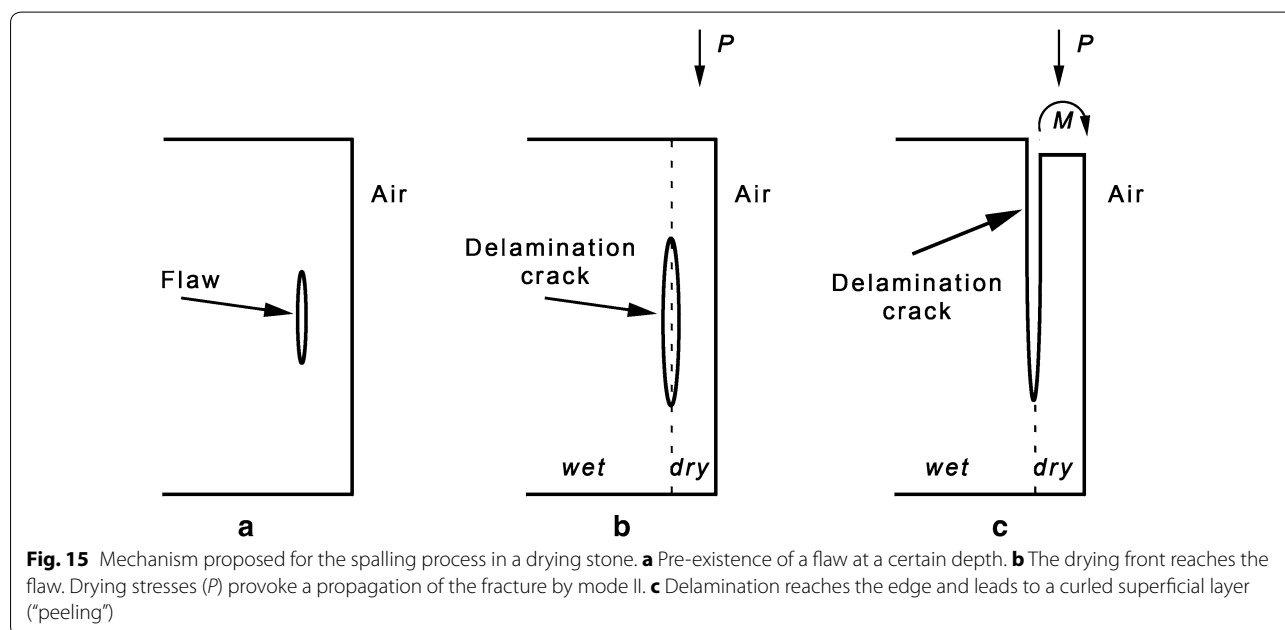
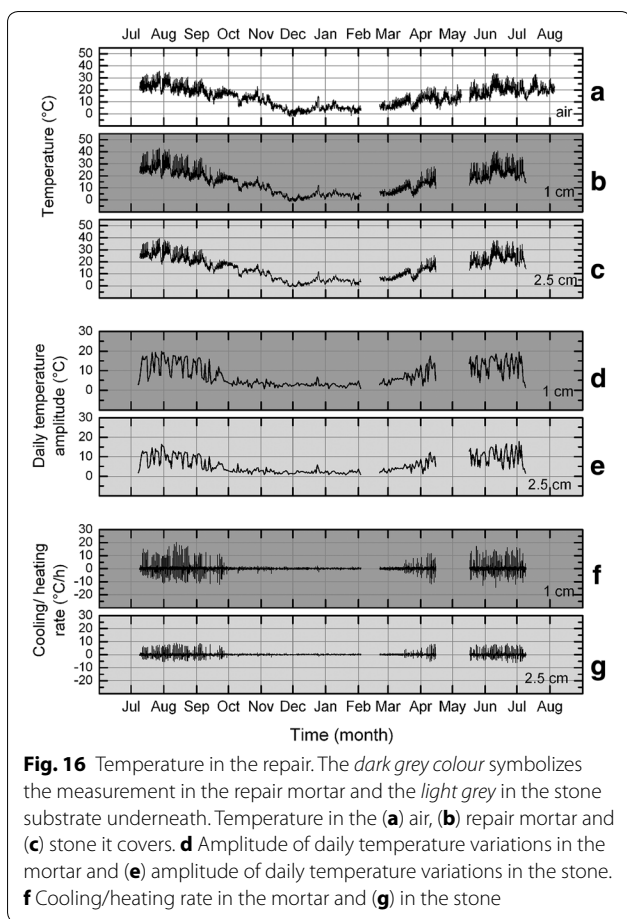


Fig. 15 Mechanism proposed for the spalling process in a drying stone. **a** Pre-existence of a flaw at a certain depth. **b** The drying front reaches the flaw. Drying stresses (P) provoke a propagation of the fracture by mode II. **c** Delamination reaches the edge and leads to a curled superficial layer ("peeling")



presented in Fig. 16d, e show that the highest variation was 19.5 °C in the repair and 17.8 °C in the natural stone.

The cooling and heating rates presented in Fig. 16f, g indicate that one of the highest heating rates in the repair layer was of 20.5 °C/h, while it was only 9.3 °C/h in the stone below it.

Owing to the viscoelasticity of the mortar, the stresses in the repair are a function of the temperature, but also of the history of seasonal and daily variations, as well as the rate at which these variations occur.

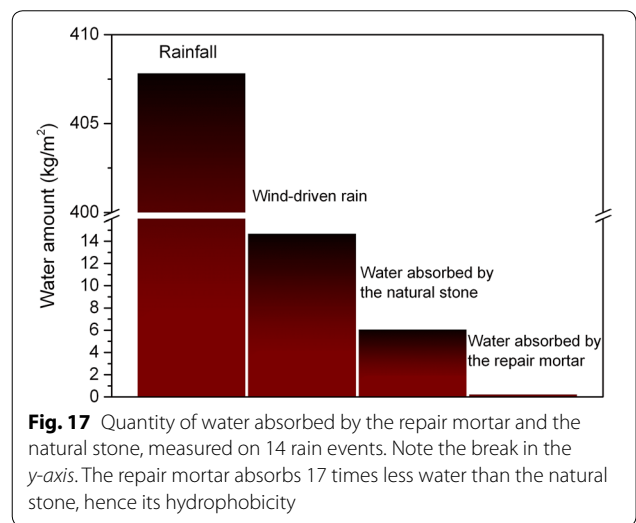
The stresses can be computed by considering all these parameters. A detailed analysis, that goes beyond the scope of this article, has been done in [20]. It shows that the magnitude of the thermal stresses alone are very small for both the repair layer and the natural stone, mainly due to the viscoelasticity of the repair material. Indeed, since its glass transition temperature is 20 °C, all the stresses that are created above this temperature are relaxed rapidly. As a consequence, and in contrast to what one might intuitively think, the highest thermal stresses are not created during summer but during the winter season. Geographical locations

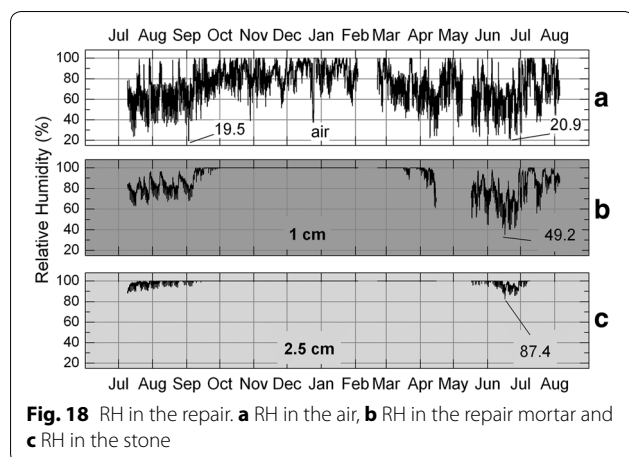
reaching particularly low temperatures are most at risk because the viscoelastic relaxation is much slower, but even in those cases damaging stresses are not expected [34].

Wind-driven rain and absorbed water

Despite the small distance between the frames collecting the wind-driven rain, the particular location of the measurement on a buttress close to the apse favours wind turbulences and provokes different rain exposures. In an attempt to quantify this difference, a non-absorbing material has been positioned to measure the wind-driven rain at the three locations during six rain events, from October 2nd to 28th, 2013. Compared to the fully non-absorbing material, the natural stone received 1.62 ± 0.35 times more and the artificial stone 1.21 ± 0.15 times more water during these rain events. These proportionality factors are used in the calculations that led to the results discussed below.

During the studied period, 3.6% of the rain was driven by the wind towards our wall (14.8 kg/m^2 of 407.9 kg/m^2 that fell on the ground during 14 distinct rain events). Of this amount, 41.8% was absorbed by the natural stone, while only 2.4% was absorbed by the artificial stone. The artificial stone thus absorbs on average 17 times less water than the natural one, despite its much higher porosity (35% against 17% for the Ostermundigen molasse). This is explained by the low affinity of water for the acrylic polymer. The results are summarized in Fig. 17. As a consequence, a large part of the rainwater driven by wind towards the artificial stone is not absorbed. It just runs off and is re-distributed down the wall. It should however be noted that the areas covered by the artificial stones are mostly very small compared to the surfaces of the natural





stone, and that not all their run-off water will be immediately absorbed by the natural stone below them. In fact, its redistribution will depend on the precipitation characteristics (rain intensity, wind) and on the respective surfaces of the natural and the artificial stones as well as their locations.

RH in the repair

The data of RH in the air, in the repair mortar and in the underlying stone at a depth of 2.5 cm are shown in Fig. 18. The data of RH at the other depths are reported in the Additional file 1.

Firstly, one can see that despite the low water absorption of the repair material, the RH of the mortar stayed at 100% during the winter months, and varied much less than the RH in the air, from 49.2 to 100%, with a maximum daily amplitude of 42%.

Secondly, in the stone below the repair mortar, the RH remained relatively constant and high, not going below 87.4% at a depth of 2.5 cm. Actually, from October to April, thus a period including autumn and winter, the RH remained at 100%. This tendency is amplified deeper in the stone. That is also the case in the non-repaired stone (“[Influence of the humidity](#)” section).

According to the measurement of hygric and hydric swelling reported in Fig. 2, over the course of one year, the stone at the interface with the repair layer could theoretically undergo a dimensional change of 1.25 mm m^{-1} which is more than two times the strain due to the temperature effect. The repair layer could experience a dimensional change of around 5 mm m^{-1} . However, as extreme as this may seem, the time-dependency of the physical properties of the mortar should be considered in the calculation of the hydric stresses, in a similar way as what has been done concerning the thermal stresses, or as in [35].

The hydric problem is nevertheless more complex owing to technical limitations of the measurement of liquid water by the sensors. Indeed, as previously mentioned, the measurement of RH does not give indications on the actual saturation degree of the materials by liquid water. Therefore, an extrapolation of a RH value of 100% to a strain value is problematic. The implementation of sensors based on impedance measurement and deployed on-site in the near future is expected to give a more appropriate answer to this question.

Apart from this issue, the swelling kinetics of the repair mortar is extremely different from that of the natural stone. As reported in Fig. 3 the natural stone swells in few minutes, while the repair material needs 3 h to reach the same value, and 4 days to reach a value of 5 mm m^{-1} .

This implies that a mismatch of swelling strain between the repair material and the stone will not be immediate, and the stresses induced can be lowered by the time-dependent mechanical properties of the mortar. Indeed, the stress relaxation that acts against the development of high thermal stresses in the mortar will also decrease the hydric stresses. Additionally, the repair mortar softens drastically when saturated with water, which will also seriously limit the development of stresses. Therefore, despite the uncertainty in the evaluation of the swelling strain mismatch, it is not expected to lead to any serious durability issues by mechanical means.

Conclusions

In the context of built heritage, measurements of temperature, relative humidity and rain events are precious pieces of information to characterize a specific environment and connect it to the observed damage morphologies. The same holds true for repaired stones, in which the repair material should be studied not only in term of material properties, but also in term of the climatic conditions to which it will be exposed, in order to maximize its compatibility.

Measurements were carried out in the natural stone and aimed at gathering information about the occurrence and the consequences of wetting and drying cycles, as well as heating and cooling events. From these measurements we mostly focussed on identifying the most extreme conditions observed to evaluate the maximum stresses that the stone may be exposed to.

The temperature variations due to the radiative heating by the sun primarily affect the first centimetre of the stone and lead to stresses of up to 1/10 the tensile strength of the stone, and are thus not expected to cause damage.

The relative humidity sensors show a high hygric content throughout the year inside the molasse sandstone. Since they only measure in the hygric regime,

and furthermore have a large inaccuracy at high RH, it is not possible to quantify the saturation degree and the associated swelling strain. The deployment of additional sensors, possibly based on impedance measurements, therefore represents an important objective for future research.

The humidity sensors used in this study could nevertheless reveal the presence of a layer of higher moisture content at a depth of 4 cm. Even though the presence of such a zone had been suspected [27], it is the first time, to the authors' knowledge, that it is experimentally reported. This layer could favour the presence of salts, localising salt crystallization at some depth below the surface and creating flaws in the stone. It is also a location where the stone would have substantially lower mechanical strength and toughness [29], and would thus be more exposed to damage.

Moreover, this high humidity level in the stone suggests that condensation is likely to occur locally within the stone, driven by temperature gradients that could favour vapour transfer towards the interior of the wall. This would impede the formation of large compressive stresses due to wetting events, which is further supported by the absence of damage morphologies characteristic of compressive stresses such as buckling.

A more common damage pattern is sanding and delamination starting from the edges of the stone blocks, and often leading to these edges having to be repaired. This observation points to a risk of tensile failure, and thus to drying stresses; a situation that the RH measurements indicate as frequent. More specifically, as drying proceeds, the depth of the drying front increases as does the depth at which pre-existing flaws parallel to the surface may be propagated to cause the type of delamination damage observed. Fast drying would exacerbate the risk posed by such situations. This explains why locations facing West are more prone to this damage, since we found that the core of the stone may remain wet for a long time over the course of the year, and that they are also subjected to warm temperatures.

A potential damage mechanism that ultimately leads to the delamination of concave plates ("peeling") is proposed. This pattern is visible in various locations on the church where the measurements were made, but also in other buildings made of this kind of stone.

Concerning the repair, the measurements provide the necessary inputs to evaluate the magnitude of the thermal stresses in the stone substrate and the repair mortar. The high temperature expansion mismatch could make one think that thermal stresses are a real threat to the type of repair considered. However, the temperatures measured show that the mortar, thanks to its viscoelastic characteristic, relieves most of the thermal stresses.

Somewhat counter-intuitively, the worst situations are in winter, because that is when the viscoelastic relaxation is the slowest [20].

The mechanical stresses linked to hygric/hydric dilatation constitute a more complex problem related to the difficulty of measuring quantitatively the water content. However, stress relaxation and substantial softening of the mortar upon wetting suggest that this will probably not lead to a critical issue for durability.

Eventually, the approach presented in this paper illustrates, for a specific monument, how the measurements needed to establish the basis for predicting the advent of such alterations may be developed. This also provides new insights into the reason for the specific scaling type of alteration pattern that is observed on clay-bearing stones throughout a rather broad range of climates.

Additional file

Additional file 1. Additional figures.

Authors' contributions

TD conducted the study, which is a part of his Ph.D. thesis focusing on the use of acrylic-based mortar for sandstone repair. He wrote the article and was involved in all the phases of the project. FG conceived the measurement system in the church of Notre-Dame de Vevey and participated in the analysis of the data. GWS and TPW participated in the mechanical analysis and the conceptualization of the damage mechanisms. RJF supervised all the phases. All authors discussed the results and implications and approved. All authors read and approved the final manuscript.

Author details

¹ Physical Chemistry of Building Materials, Institute for Building Materials, HIF, ETH Zurich, 8093 Zurich, Switzerland. ² RINO Sarl, 1807 Blonay, Switzerland. ³ Department of Civil and Environmental Engineering, Eng. Quad. E-319, Princeton University, Princeton, NJ 08544, USA.

Acknowledgements

The authors would like to thank the parish of Notre-Dame de Vevey for authorizing access to the church.

Competing interests

The authors declare that they have no competing interests.

Received: 25 May 2016 Accepted: 8 October 2016

Published online: 11 November 2016

References

1. Wangler T. Swelling clay and its inhibition in the Villarod molasse. In: Science and art: a Future for Stone. Proceedings of the 13th international congress on the deterioration and conservation of stone, vol 1. Paisley; 2016. pp. 189–196.
2. Kündig R, Mumenthaler T, Eckardt P, Keusen HR, Schindler C, Hofmann F, Vogler R, Guntli P. Die mineralischen Rohstoffe der Schweiz. Zurich: Schweizerische Geotechnische Kommission; 1997.
3. Félix C. Comportement des grès utilisés en construction sur le Plateau suisse. In: Symposium international AIGI, la géologie de l'ingénieur appliquée à l'étude, à la préservation et à la protection du patrimoine historique. Athens, Greece, 19–23; 1988. pp. 833–841.

4. Furlan V, Félix C, Girardet F, Indermühle Y, Engler M, Pancella R, Citti M, Disantolo A. Recueil des publications LCP 1975–1995: matériaux de construction, pierre, pollution atmosphérique, peinture murale. Lausanne: Ecole Polytechnique Fédérale de Lausanne; 1996.
5. Jiménez-González I, Scherer GW. Effect of swelling inhibitors on the swelling and stress relaxation of clay bearing stones. *Environ Geol*. 2004;46(3–4):364–77.
6. Félix C. Choix de grès tendre du Plateau suisse pour les travaux de conservation. In: Proceedings of the LCP Congress, preservation and restoration of cultural heritage, Montreux, 24–29; 1995. p. 1995.
7. Anson Cartwright T, Vergès-Belmin V. Illustrated glossary on stone deterioration patterns. Paris: ICOMOS; 2008.
8. De Quervain F. Verhalten der Bausteine gegen Witterungseinflüsse in der Schweiz. In: Beiträge zur Geologie der Schweiz. Geotechnische Serie. Bern: Kümmerly & Frey; 1951. p. 65.
9. Zehnder K. Weathering of molasse sandstones on monuments and natural outcrops. In: 3rd International congress on deterioration and preservation of stones. Venice, 24–27; 1979.
10. Zehnder K. Verwitterung von Molassesandsteinen an Bauwerken und in Naturaufschlüssen. Kümmerli & Bern: Schweizerische Geotechnische Kommission; 1982.
11. Rousset B. La molasse grise de Lausanne: de la roche sédimentaire détritique au matériau de construction séculaire. In: Déontologie de la pierre: stratégies d'intervention pour la cathédrale de Lausanne, 31 mai 2012; 2012. pp. 12–17.
12. Amsler C. Une cathédrale de molasse: Lausanne, expériences et perspectives. In: Proceedings of the LCP Congress, PRESERVATION and restoration of cultural heritage, Montreux, 24–29; 1995. pp. 29–44.
13. Furlan V, Girardet F. Pollution atmosphérique et dégradation de la molasse. *Chantiers/Suisse*. 1983;14:989–94.
14. Torney C, Forster AM, Kennedy CJ, Hyslop EK. Plastic repair of natural stone in Scotland: perceptions and practice. *Struct Surv*. 2012;30(4):297–311.
15. Rossi-Doria PR. Mortars for restoration: basic requirements and quality control. *Mater Struct*. 1986;19(6):445–8.
16. Committee RT. RILEM TC 203-RHM: repair mortars for historic masonry—performance requirements. *Mater Struct*. 2012;45(9):1277–85.
17. Isebaert A, Van Parys L, Cnudde V. Composition and compatibility requirements of mineral repair mortars for stone—a review. *Constr Build Mater*. 2014;59:39–50.
18. Jiménez-González I, Rodríguez-Navarro C, Scherer GW. Role of clay minerals in the physicomaterial deterioration of sandstone. *J Geophys Res*. 2008;113:82.
19. Ettel WP. Kunstharze und Kunststoff-dispersionen für Mörtel und Betone. Düsseldorf: Beton-Verlag; 1998.
20. Demoulin T, Scherer GW, Girardet F, Flatt RJ. Thermo-mechanical compatibility of viscoelastic mortars for stone repair. *Mater (Basel)*. 2016;9(1):56.
21. Hall K. The role of thermal stress fatigue in the breakdown of rock in cold regions. *Geomorphology*. 1999;31(1–4):47–63.
22. Camuffo D. Microclimate for cultural heritage, 2nd ed. Conservation, restoration, and maintenance of indoor and outdoor monuments. San Diego: Elsevier Science Ltd; 2013.
23. Al-Omari A, Brunetaud X, Beck K, Al-Mukhtar M. Hygrothermal stress and damage risk in the stones of the Castle of Chambord-France. *Int J Civ Struct Eng*. 2014;4(3):402–18.
24. Krüger M. Long-term wireless monitoring of historic structures—lessons learned from practical applications. In: Proceedings of the 6th European workshop on structural health monitoring, Sept. 26 to 28th 2011. Berlin; 2012. pp. 1–9.
25. Smith BJ, Srinivasan S, Gomez-Heras M, Basheer M, Viles H. Near-surface temperature cycling of stone and its implications for scales of surface deterioration. *Geomorphology*. 2011;130(1–2):76–82.
26. Ruedrich J, Bartelsen T, Dohrmann R, Siegesmund S. Moisture expansion as a deterioration factor for sandstone used in buildings. *Environ Earth Sci*. 2010;63(7–8):1545–64.
27. Snethlage R, Wendler E. Moisture cycles and sandstone degradation. In: Baer NS, Snethlage R, editors. Dahlem workshop on saving our architectural heritage, the conservation of historic stone structures. Berlin: Wiley; 1997. p. 7–24.
28. Siedel H, Pfefferkorn S, Vonplehwe-Leisen E, Leisen H. Sandstone weathering in tropical climate: results of low-destructive investigations at the temple of Angkor Wat. Cambodia. *Eng Geol*. 2010;115(3–4):182–92.
29. Nara Y, Morimoto K, Hiroyoshi N, Yoneda T, Kaneko K, Benson PM. Influence of relative humidity on fracture toughness of rock: implications for subcritical crack growth. *Int J Solids Struct*. 2012;49(18):2471–81.
30. Zerbi S. Construction en pierre massive en Suisse. Ecole Polytechnique Fédérale de Lausanne EPFL; 2011.
31. Wangler TP, Stratulat A, Duffus P, Prevost JH, Scherer GW. Flaw propagation and buckling in clay-bearing sandstones. *Environ Earth Sci*. 2010;63(7–8):1565–72.
32. Bohn S, Pauchard L, Couder Y. Hierarchical crack pattern as formed by successive domain divisions. I. Temporal and geometrical hierarchy. *Phys Rev E Stat Nonlin Soft Matter Phys* 2005;71(4 Pt 2): 046214.
33. Style RW, Peppin SSL, Cocks ACF. Mud peeling and horizontal crack formation in drying clays. *J Geophys Res Earth Surf*. 2011;116:11.
34. Demoulin T, Scherer GW, Girardet F, Flatt RJ. Acrylic-based mortar for stone repair: a viscoelastic analysis of the thermal stresses, In: 13th International congress on the deterioration and conservation of stone, 6–10 September 2016. Glasgow, Scotland.
35. Scherer GW, Jimenez Gonzalez I. Characterization of swelling in clay-bearing stone. *Geol Soc Am*. 2005;390:51–61.

Submit your manuscript to a SpringerOpen® journal and benefit from:

- Convenient online submission
- Rigorous peer review
- Immediate publication on acceptance
- Open access: articles freely available online
- High visibility within the field
- Retaining the copyright to your article

Submit your next manuscript at ► springeropen.com
